Mapping Cortical and Subcortical Asymmetry in Obsessive-Compulsive Disorder: Findings From the ENIGMA Consortium

Supplement 1

Supplemental Methods and Materials

Datasets. The datasets used in this study were provided by members of the OCD Working Group within the ENIGMA Consortium (1). There were 46 independent datasets from 16 countries (Brazil, Canada, China, Germany, India, Italy, Japan, the Netherlands, Portugal, Republic of Korea, Sweden, South-Africa, Spain, Switzerland, United Kingdom, and United States of America). Data comprised both subcortical and cortical measures from a total of 2278 patients with OCD and 2093 healthy control subjects (16 pediatric datasets comprising 501 OCD patients and 439 healthy controls, and 30 adult datasets comprising 1777 OCD patients and 1654 healthy controls). Thirty-five and thirty-eight of these datasets were identical to those included in the previous ENIGMA subcortical (2) and cortical (3) studies respectively. Handedness information was not extensive within these datasets, but previous large-scale analyses in datasets of over 15,000 healthy subjects have indicated that handedness is of little relevance to the structural brain asymmetry measures analyzed here (4, 5). Basic demographic and clinical information are summarized in Table 1 and Figure S1-2; more details of the contributing datasets can be found in Table S1. All local institutional reviews boards permitted the use of extracted measures from their anonymized data. In addition, we leveraged publicly available summary statistics which describe the average form of brain regional asymmetries, based on our previous larger studies of healthy individuals (http://conxz.github.io/neurohemi; (4, 5)).

Image Acquisition and Processing. Structural T1-weighted MRI scans were acquired and processed locally at each collection site. Images were acquired at different field strengths (1.5 T and 3T). All images were analyzed using one automated and validated pipeline, i.e. “recon-all” as implemented in *FreeSurfer* (version 5.3). Briefly, the main stages of the processing pipeline include normalization of brain signal intensity, skull-stripping, white matter and gray matter segmentation, and delineation of the

gray-white interface (inner surface) and the pial surface (outer surface). Next, the surface is divided into separate cortical regions using an automated labeling approach, where not only location information based on a probabilistic surface-based atlas, but also local curvature and contextual information (e.g., sulcal and gyral geometry) of subject-specific surface are taken into consideration. Finally, for each subject, surface area and mean thickness was extracted for each of the 68 cortical regions (34 per hemisphere) in the Desikan-Killiany parcellation scheme (6), as well as total hemispheric surface area, and the average mean thickness over each hemisphere. We chose this parcellation scheme because it is well-established in the surface space, has been widely used in brain structure studies including previous ENIGMA consortium studies, and is feasible for large collaborative projects (see e.g. (5)). For more details on the image processing and data collection, please refer to (2, 3, 6). In addition, volumes of eight subcortical regions of interest, including seven subcortical structures (nucleus accumbens, amygdala, caudate, hippocampus, pallidum, putamen, and thalamus), and the lateral ventricle volume, were calculated. This segmentation is also part of the pipeline 'recon-all', and based on an atlas containing probabilistic information on the location of structures (7). All calculations were made in each subject's native space. Further processing and quality control for all datasets was then performed following standardized ENIGMA protocols (http://enigma.ini.usc.edu/protocols/imaging-protocols/), which include, briefly, extracting cortical and subcortical measures from *FreeSurfer* outputs, outlier detection, and visual quality checking. Finally, each dataset was prepared based on a unified table format, and shared with the central analysis team for this study.

Asymmetry Indexes. The main aim of this study was to investigate differences in subcortical and cortical asymmetry related to OCD. To this end, for each participant, and each subcortical or cortical measure, an Asymmetry Index (AI) was defined as *(L-R)/((L+R)/2)*, where L and R represent the corresponding left and right volume measures (from subcortical regions), or thickness and surface area measures (from cortical regions). Thus, positive and negative AI values indicate leftward and rightward asymmetry, respectively, for a given left-right paired measure. This AI formula has been widely used in previous brain asymmetry studies (8-10), including our own (4, 5, 11). In addition, it is important to note that in the definition of the AI, the difference (i.e., L-R) was normalized by use of the bilateral

measures as denominator (i.e., L+R), such that the measure does not scale with the overall magnitude of L and R. For this reason, we also did not adjust for intracranial volume (ICV) in our analyses. We previously showed that there are subtle associations between ICV and regional brain asymmetries in the general population (5). However, here we wished to capture the full extent of any OCD-asymmetry associations, regardless of whether underlying causal influences might also affect ICV. Therefore, we did not adjust for ICV in our main analysis. Nonetheless, we also repeated our analyses including ICV as a covariate effect, to confirm that results did not depend on this choice (Results are shown below).

In our main analyses, we did not exclude any data points in addition to those already excluded by the quality control procedures included in the ENIGMA protocols (see (2, 3) for further details on quality checking). However, we also repeated our analyses after excluding possible outliers on each AI, within each dataset and each diagnosis group, with a threshold of 2.5SD from the mean, in order to confirm that findings from the main analysis were not driven by extreme data points.

Case-control Analyses. Separately for the pediatric and adult data, and for each subcortical or cortical AI, we pooled data from all available individuals from each dataset, and used a mega-analytical framework to investigate the case-control effects. Specifically, for each AI, we used a linear mixed-effect model (using *lme4* R package, version 1.1-12), with AI as the outcome variable, and a binary indicator of diagnosis (0=healthy controls, 1=OCD patients) as the predictor of interest. In each model, a binary variable for sex, and a continuous measure for age (in years at time of scan) were included as confounding factors, and the categorical variable ‘dataset’ as a random-effect term. Model fit was checked visually by inspection of the plot of residuals versus fitted values, and the histogram and quantile-quantile (Q-Q) plots for the residual values. Condition number (i.e., Kappa) and variance inflation factor (VIF) were calculated in order to assess collinearity (troubling collinearity is indicated by Kappa values of 30, and/or VIF values of 5 or above). Coefficients of “Estimate”, “Std. Error”, and “t value” for the predictor of interest (i.e., diagnosis) were extracted from the model outputs, while significance (i.e., *p* value) was assessed using likelihood ratio tests to compare models with and without the predictor (using function *anova* from *stats* R package, version 3.2.5). Separately within each age

group (pediatric or adult), and separately for each type of asymmetry measure, i.e. 8 tests for subcortical volume AIs, 35 tests for cortical thickness AIs, 35 tests for cortical surface area AIs, the false-discovery-rate (FDR) correction procedure ($q <= 0.05$) was used to correct for multiple comparisons. Cohen's *d*, as effect size, was calculated for each effect based on its *t* value and the sample sizes (i.e., *N1* and *N2*) of each group, with the formula *t*sqrt(1/N1+1/N2)* (12). To investigate whether the effect sizes of diagnosis on cortical AIs were related between the pediatric and adult data, we calculated the correlations between the Cohen's d across all 34 cortical regions, separately for cortical thickness and surface area AIs.

We repeated the main analysis by additionally including age^2 as a confounding factor, in case of substantial non-linear effects on AIs (but this had very little effect, see Results). We also repeated the main analyses with regard to potential influences of MRI scanner field strength. In this analysis, in addition to sex and age, an additional binary predictor variable of scanner field strength (1.5T scanners versus 3T scanners) was included. We were interested in whether 1) scanner effects on the AIs were significant, and 2) whether any significant effects of diagnosis on AIs remained after controlling for effects related to differences in scanner field strength.

Separately for thickness and surface area, we additionally calculated an overall 'typicality score' per subject, which indexed how much a given subject deviated from the population mean asymmetry profile, when considered simultaneously across all 34 cortical regions. The typicality score for a given subject was calculated as the Spearman correlation coefficient between that the subject's AIs and the population mean AIs, across all 34 regions. Population data were based on summary statistics from more than 17,000 subjects drawn from the general population or healthy control datasets, which were available online (http://conxz.github.io/neurohemi; (5)). A lower typicality score indicates more deviation from the mean asymmetry profile in the population. We compared the typicality scores between OCD patients and controls, using the same linear mixed-effect model as used in the main analyses (i.e. correcting for sex, age and dataset), except that the outcome variable was now the typicality score. The hypothesis was that the overall asymmetry profile in OCD, as considered across multiple regions, might deviate from

the typical pattern more than for the control subjects in this study. No multiple testing correction was performed, as this was intended as an exploratory analysis.

OCD Case-only Analyses of Clinical Characteristics. For AIs which were potentially associated with OCD in the main analysis (see Results), we further investigated, within cases only, whether the following predictors were associated with the AIs: medication status (medication-free OCD cases vs. medicated cases), age at disease onset (in years), disease duration (in years), current anxiety comorbidity (categorical yes/no) and current depression comorbidity (categorical yes/no). In addition, we also tested these AIs in relation to OCD severity measures, which were the total score based on the Yale-Brown Obsessive Compulsive Scale (Y-BOCS) or Children's Yale-Brown Obsessive Compulsive Scale (CY-BOCS), and the absence or presence of 5 previously identified symptom dimensions derived from the Y-BOCS (or CY-BOCS) symptom checklist: aggression/checking; cleaning/contamination; sexual/religion; hoarding; ordering/symmetry (13-15). For more details of this scheme, please refer to (2, 3). Data for these case-only variables were available for the majority of cases (see Supplementary Table S1 for the available sample sizes within each dataset). The same linear mixed-effect model was used as the main analysis, again with AI as the outcome variable, except that the predictor variable 'diagnosis' was now replaced by one of the within-case predictor variables per model (e.g. medicated/unmedicated as a binary variable, age of onset as a continuous variable etc.). All case-only analyses were performed separately for each age groups (pediatric and adult). These post-hoc analyses were intended as purely exploratory, and no correction for multiple testing was applied.

Supplemental Results

Main Results for Adult Data. Regionally, only the postcentral gyrus showed a nominally significant AI difference between patients and controls, which involved both its thickness AI ($t = -2.10$, $p = 0.036$, $d = -0.073$) and surface area AI ($t = -2.12$, $p = 0.034$, $d = -0.074$), but these effects could not survive correction for multiple testing. No other case-control comparisons of either subcortical or cortical AIs showed significant effects in the adult data (uncorrected ps >0.05).

When repeating the main analysis including age2 additionally in the model, all of the Cohen's d for the effects of diagnosis remained within 0.005 of their values before having included age2, and the same AI (adult global surface area) remained significant after FDR correction. None of the AIs showed significant scanner effects in the adult data (ps >0.05), and the effect of diagnosis on the global surface area AI remained when adding scanner field strength as a predictor variable to the model (diagnosis t = -2.44, p = 0.015, d = -0.085).

Additional Analyses. Our previous large-scale study has shown significant relationships between ICV and brain asymmetries, although the effect sizes are subtle (5). We repeated our analyses after additionally adjusting for ICV. Results showed that the main results remained: pediatric thalamus volume asymmetry: t = 2.85, p = 0.0045, d = 0.19; pediatric pallidum volume asymmetry: t = -3.07, p = 0.0022, d = -0.20; adult global hemispheric surface area asymmetry: t = -2.43, p = 0.015, d = -0.85). These findings suggest that adjusting for ICV had little impact on OCD case-control differences in brain asymmetries.

Regarding the adult OCD patients, the previous study showed a larger pallidum (again left plus right) than controls, driven by patients with a childhood-onset of disease (2). But we saw no significant effects on the asymmetry of this structure in the adult patients. We repeated our analyses with data for each subgroup of age of onset of disease: early-onset (i.e., before 18 years old) and late-onset patients (i.e., after 18 years old). No significant differences were found in either subgroup. Specifically, in the early-onset subgroup, neither asymmetry of the thalamus or pallidum showed significant differences (thalamus: t = 1.37, p = 0.17; pallidum: t = -0.028, p = 0.98). Similar null results were found in the late-onset subgroup (thalamus: t = 1.82, p = 0.07; pallidum: t = -0.48, p = 0.63). We further compared the effects between two subgroups, and found no significant differences (thalamus: t = 1.56, p = 0.12; pallidum: t = -0.088, p = 0.93).

Supplemental Tables

All supplemental tables (Tables S1-S7) are available in a separate Excel file.

Supplemental Figures

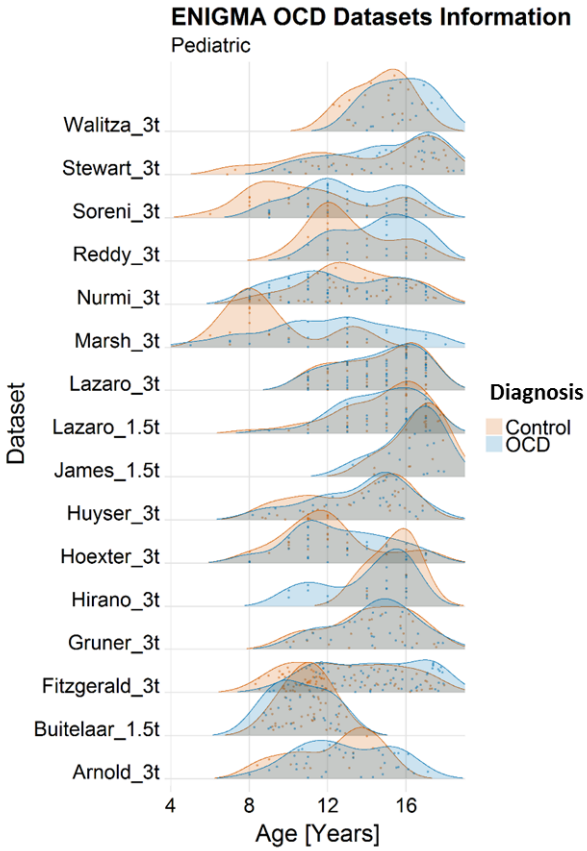

Figure S1. Age distributions of participants in each pediatric dataset.

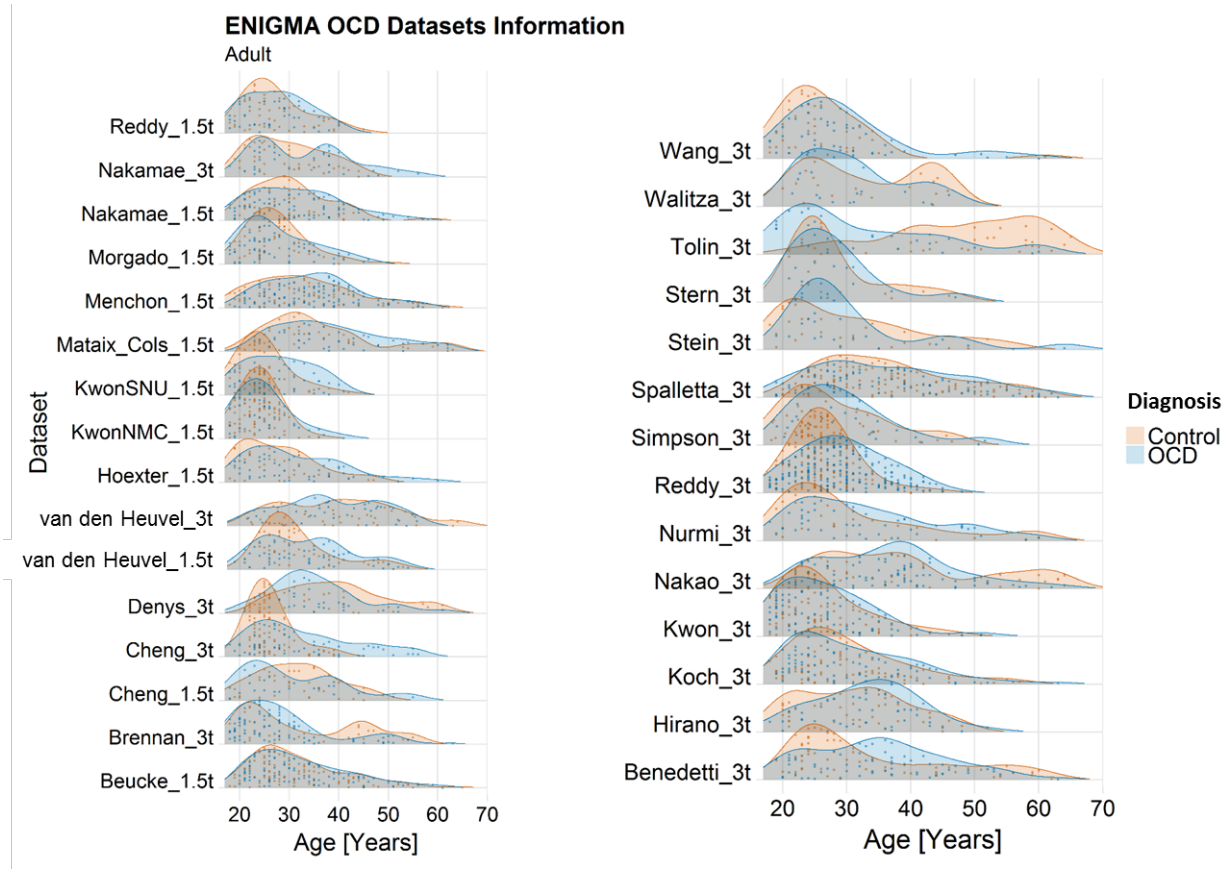

Figure S2. Age distributions of participants in each adult dataset.

Supplemental References

1. Thompson PM, Stein JL, Medland SE, Hibar DP, Vasquez AA, Renteria ME, et al. (2014): The ENIGMA Consortium: large-scale collaborative analyses of neuroimaging and genetic data. *Brain imaging and behavior*. 8:153-182.
2. Boedhoe P, Schmaal L, Abe Y, Ameis SH, Arnold PD, Batistuzzo MC, et al. (2017): Distinct Subcortical Volume Alterations in Pediatric and Adult OCD: A Worldwide Meta- and Mega-Analysis. *Am J Psychiatry*. 174:60-69.
3. Boedhoe P, Schmaal L, Abe Y, Alonso P, Ameis SH, Anticevic A, et al. (2018): Cortical Abnormalities Associated With Pediatric and Adult Obsessive-Compulsive Disorder: Findings From the ENIGMA Obsessive-Compulsive Disorder Working Group. *Am J Psychiatry*. 175:453-462.
4. Guadalupe T, Mathias SR, vanErp TG, Whelan CD, Zwiers MP, Abe Y, et al. (2016): Human subcortical brain asymmetries in 15,847 people worldwide reveal effects of age and sex. *Brain Imaging Behav*.
5. Kong X-Z, Mathias SR, Guadalupe T, Group ELW, Glahn DC, Franke B, et al. (2018): Mapping cortical brain asymmetry in 17,141 healthy individuals worldwide via the ENIGMA Consortium. *PNAS*.
6. Desikan RS, Segonne F, Fischl B, Quinn BT, Dickerson BC, Blacker D, et al. (2006): An automated labeling system for subdividing the human cerebral cortex on MRI scans into gyral based regions of interest. *Neuroimage*. 31:968-980.
7. Fischl B, Salat DH, Busa E, Albert M, Dieterich M, Haselgrove C, et al. (2002): Whole brain segmentation: Automated labeling of neuroanatomical structures in the human brain. *Neuron*. 33:341-355.
8. Kurth F, Gaser C, Luders E (2015): A 12-step user guide for analyzing voxel-wise gray matter asymmetries in statistical parametric mapping (SPM). *Nature Protocols*. 10:293-304.
9. Leroy F, Cai Q, Bogart SL, Dubois J, Coulon O, Monzalvo K, et al. (2015): New human-specific brain landmark: the depth asymmetry of superior temporal sulcus. *Proc Natl Acad Sci U S A*. 112:1208-1213.
10. Zhong S, He Y, Shu H, Gong G (2017): Developmental Changes in Topological Asymmetry Between Hemispheric Brain White Matter Networks from Adolescence to Young Adulthood. *Cereb Cortex*. 27:2560-2570.
11. Zhen Z, Kong XZ, Huang L, Yang Z, Wang X, Hao X, et al. (2017): Quantifying the variability of scene-selective regions: Interindividual, interhemispheric, and sex differences. *Hum Brain Mapp*. 38:2260-2275.
12. Nakagawa S, Cuthill IC (2007): Effect size, confidence interval and statistical significance: a practical guide for biologists. *Biological reviews of the Cambridge Philosophical Society*. 82:591-605.
13. Scahill L, Riddle MA, McSwiggin-Hardin M, Ort SI, King RA, Goodman WK, et al. (1997): Children's Yale-Brown Obsessive Compulsive Scale: reliability and validity. *J Am Acad Child Adolesc Psychiatry*. 36:844-852.
14. Goodman WK, Price LH, Rasmussen SA, Mazure C, Fleischmann RL, Hill CL, et al. (1989): The Yale-Brown Obsessive Compulsive Scale. I. Development, use, and reliability. *Arch Gen Psychiatry*. 46:1006-1011.
15. Mataix-Cols D, Fullana MA, Alonso P, Menchon JM, Vallejo J (2004): Convergent and discriminant validity of the Yale-Brown Obsessive-Compulsive Scale Symptom Checklist. *Psychother Psychosom*. 73:190-196.